Wang, L., Chen, C., Thomas, M., Kaban, M. K., Güntner, A., Du, J. (2018): Increased water storage of Lake Qinghai during 2004 to 2012 from GRACE data, hydrological models, radar altimetry, and in-situ measurements. - *Geophysical Journal International*, *212*, 1, pp. 679—693.

DOI: http://doi.org/10.1093/gji/ggx443

Geophysical Journal International

Geophys. J. Int. (2018) **212,** 679–693
Advance Access publication 2017 October 14
GJI Gravity, geodesy and tides

doi: 10.1093/gji/ggx443

Increased water storage of Lake Qinghai during 2004–2012 from GRACE data, hydrological models, radar altimetry and *in situ* measurements

Linsong Wang,[1] Chao Chen,[1] Maik Thomas,[2,3] Mikhail K. Kaban,[2] Andreas Güntner[2] and Jinsong Du[1]

[1]*Hubei Subsurface Multi-scale Imaging Key Laboratory, Institute of Geophysics and Geomatics, China University of Geosciences, Wuhan* 430074*, Hubei, China. E-mail: wanglinsong@cug.edu.cn*
[2]*Helmholtz Centre Potsdam, GFZ German Research Centre for Geosciences, Telegrafenberg, D*-14473 *Potsdam, Germany*
[3]*Freie Universität Berlin, Institute of Meteorology, D*-14195 *Berlin, Germany*

Accepted 2017 October 13. Received 2017 October 4; in original form 2016 December 16

SUMMARY

Terrestrial water storage (TWS) changes in the Tibetan Plateau (TP) are sensitive indicators for water dynamics associated with climate variability. Joint analyses using both GRACE space mission and satellite altimetry data are increasingly being used to monitor TWS. The objective of this study is to confirm that it is possible to reliably monitor water storage changes in large lakes based on integrative analysis of GRACE data. This study focuses on data integrated and analysed for Lake Qinghai located in the northeast TP, and shows a clear continuous water-level rise since 2004. We have developed a simple framework to estimate water storage variations in individual regions using a spatial averaging kernel, while simultaneously minimizing the effects resulting from uncertainties of GRACE data using Land Surface Models (LSMs) and *in situ* measurements. Water storage anomalies not related to lakes, such as soil moisture, snow and reservoirs, are estimated using GLDAS/Noah and reservoir gauge station for the period 2004–2012. Our results show that the rate of rise in mass of the GRACE-derived TWS (post GLDAS/Noah anomaly removal) is calculated to be 0.27 ± 0.12 cm yr^{-1}, or an average water-level increase rate of 0.20 ± 0.09 m yr^{-1} after GRACE-derived TWS (i.e. 0.27 ± 0.12 cm yr^{-1}) multiplied by 1/1.34 to recover the 'real' mass variation signal using scaling factor method based on basin function from grids of Lake Qinghai from 2004 to 2012, which is equivalent to the volume change 0.86 ± 0.37 km^3 yr^{-1} and mainly caused by the fast expansion of Lake Qinghai (0.44 ± 0.04 km^3 yr^{-1} from altimetry/*in situ* measurements) and impoundment of Longyangxia reservoir (0.28 ± 0.17 km^3 yr^{-1} based on the linear height–volume relationship and *in situ* water-level observations). The residual signal (GRACE−GLDAS/Noah−reservoir−Lake Qinghai) likely reflects the mass leakage from the surrounding lakes in the regions (i.e. Har, Gyaring and Ngoring) and groundwater contributions (i.e. groundwater is not included in GLDAS/Noah) due to the limited spatial resolution of GRACE. The results suggest that the combined use of LSM and GRACE measurements is a useful method for monitoring changes in the mass of large lakes. Additionally, our analysis shows that it is necessary to improve LSM results with *in situ* forcing parameters and groundwater level data, which will reduce the uncertainty in the application of GRACE data. There is still a need to use complementary models or *in situ* observations to eliminate the influence of glacial isostatic adjustments and tectonic processes.

Key words: Hydrology; Satellite geodesy; Satellite gravity; Time variable gravity.

1 INTRODUCTION

As a part of the natural land-water cycle, changes in lake system hydrology provide important information on regional impacts of global climate change. The Tibetan Plateau (TP), known as the 'Third Pole' of the Earth and the 'Asian water tower', has experienced impacts from climate change due to global warming in recent decades (Lu *et al*. 2005; Qiu 2008; Immerzeel *et al*. 2010).

The TP has an average elevation of more than 4000 m above sea level, and contains many mountain glaciers, which are important contributors to both the growth of regional lakes (Liu *et al*. 2009; Zhang *et al*. 2011a; Song *et al*. 2014) and global mean sea level rise (Jacob *et al*. 2012; Gardner *et al*. 2013). The TP covers numerous lakes with a total area of 4.07×10^4 km^2 (Zhang *et al*. 2013). Previous studies have investigated changes in lake level and size which are associated with accelerated glacier melting (Yao *et al*. 2007; Kang *et al*. 2009; Zhu *et al*. 2010; Song & Sheng 2016), changes in the energy and water cycles (Yang *et al*. 2011, 2013; Unger-Shayesteh *et al*. 2013) and ecosystem (Li *et al*. 2008; You *et al*. 2008). Other researches have focused on explaining the factors driving these changes, specifically glacial meltwater supply caused by global warming and climate-driven precipitation and evaporation changes. Regional changes in these factors can be observed via the spatial and temporal variability of the lakes in different regions of the TP, as many large lakes in the central TP have expanded, since the 1970s (Huang *et al*. 2011; Liao *et al*. 2012; Song *et al*. 2014), while some lakes demonstrate a decrease in mass in the southern TP (Ye *et al*. 2007; Zhang *et al*. 2011a).

Lake Qinghai, located in the northeast TP, is the largest salt lake in China (average salinity $\sim$12.5 g L^{-1}) and grew differently compared with most other regional lakes, for example, significant shrinkage from the 1950s to 1990s and expansion in the 2000s (Song *et al*. 2013). Numerous earlier studies have attempted to monitor water level and area fluctuations of Lake Qinghai using remote sensing techniques including ICESat (Ice, Cloud and land Elevation Satellite) altimetry data and Landsat Thematic Mapper (TM)/Enhanced Thematic Mapper Plus(ETM+) images (Zhang *et al*. 2011a; Phan *et al*. 2012; Wang *et al*. 2013). In addition to traditional gauge data, water-level changes derived from satellite altimetry data are especially important for the management of water resources affected by climate change. Continuous monitoring provides some parameters of the mass changes in Lake Qinghai, such as the water level, surface area and volume variation based on several satellite altimetry missions (LEGOS/GOHS—Laboratoire d'Etudes en Geodesie et Oceanographie Spatiales, Equipe Geodesie, Oceanographie, et Hydrologie Spatiales), however, high-quality satellite images and data are not sufficient to estimate the total vertically integrated water content from the surface to underground (e.g. surface water, groundwater and soil moisture, etc.), or the total mass balance in the lake (Song *et al*. 2013).

Global-scale mass variations related to changes in terrestrial water storage (TWS) are visible in the time-variable gravity field provided by the GRACE satellite mission. Changes in total water storage (ΔtotalWS) monitored by GRACE are sensitive to the TWS integrated through the entire water column. This includes surface water storage (ΔSurWS), soil moisture storage (ΔSMS), snow water storage (ΔSnWS) and groundwater storage (ΔGWS):

$$\Delta\text{totalWS} = \Delta\text{SurWS} + \Delta\text{SMS} + \Delta\text{SnWS} + \Delta\text{GWS} \quad (1)$$

These water storage changes are generally expressed in terms of an Equivalent Water Height (EWH: volume/area of water thickness) or water volume in a basin. Based on these data, several previous studies have revealed changes in the mass balance in the Inner Tibet Plateau and in the High Mountain Asia (HMA) during the last decade (Matsuo & Heki 2010; Yi & Sun 2014).

The gravity signal of individual regions can be isolated from GRACE gravity coefficients using spatial averaging of kernel, while simultaneously minimizing the effects of observational errors and contamination from surrounding glacial, hydrological and oceanic gravity signals (Swenson & Wahr 2002). Thus, extracting regional mass anomalies from GRACE data is useful for evaluating changes in the distribution of water in large lakes, as has been done in the great lakes region of East Africa (Swenson & Wahr 2009; Becker *et al*. 2010). To confirm the observed gravity increase in the TP being primarily caused by lake storage gain, Wang *et al*. (2016) compared GRACE and ICESat observations across four subregions of the TP and found an abrupt change in water level of many lakes (i.e. Yaggain Co, Kyebxang Co, Zige Tang Co and Lake Qinghai) in the northeastern region. Importantly, the recent study indicate the ability of GRACE to detect water storage changes in the Longyangxia Reservoir, which shows GRACE data have promising potential in detecting water storage changes in this $\sim$400 km^2 reservoir or a small signal size is not a restricting factor for detection using GRACE data (Yi *et al*. 2017).

While there have been many large-scale regional studies of changes in lake mass, GRACE-based studies examining changes in water storage in specific lakes such as Lake Qinghai are few. One reason is that GRACE observations reflect a sum of many superimposed effects, which are difficult to separate in the data (Song *et al*. 2015). In other words, GRACE cannot distinguish between anomalies resulting from different components of ΔtotalWS. Another reason is due to the limited spatial horizontal resolution of post-processed GRACE solutions, which is on the order of $\sim$300 km and represents an averaging effect which may be different from point measurements (Swenson & Wahr 2002). To improve the horizontal and vertical resolutions of GRACE data in Land Surface Model (LSM) outputs, the scaling factor approach is used to rescale the TWS estimates (Landerer & Swenson 2012; Long *et al*. 2015), and individual components such as groundwater are extracted from GRACE-derived TWS minus the LSM estimates (Rodell *et al*. 2009; Scanlon *et al*. 2012; Feng *et al*. 2013). Even with these techniques, LSM applications still have significant uncertainty problems such as the lack of model forcing inputs calibrated against *in situ* measurements, which restricts the comparative analysis in the TP.

This study focuses on Lake Qinghai (Fig. 1), for which we develop a simple framework to estimate water storage variations in individual regions while simultaneously minimizing the effects resulting from uncertainties of GRACE observations and other factors related to the surrounding glacial, snow, hydrological and anthropogenic signals. Significant mass changes of Lake Qinghai have occurred after the launch of the GRACE mission in 2002. The water level of Lake Qinghai has increased by $\sim$1 m from 2004 to 2012. We try to demonstrate the potential of applying GRACE measurements to detect mass changes in the larger lakes such as Lake Qinghai basin (area size is about 200 km $\times$ 200 km, which is smaller than the GRACE footprint size $\sim$300 km). Spatial averaging kernel is created to isolate the gravity signal of GRACE from the signals outside the lake and minimize leakage effects from the lake. In order to improve the vertical resolution of GRACE, we test three LSMs to select the optimal hydrological model based on LSMs outputs compare with the results derived by GRACE, and LSMs inputs compare with *in situ* measurements from the weather stations. The monthly simulation of the TWS changes excluding lake storage is used to remove the effects of the water storage adjacent to Lake Qinghai, and *in situ* measurements of the water level are used to remove the influence of the constructed Longyangxia reservoir dam. Furthermore, we comparatively analyse results of previous studies based on *in situ* and satellite altimetry measurements, and the GRACE-observed mass anomalies associated with the fluctuation of Lake Qinghai. Finally, we discuss the relationship between the forcing

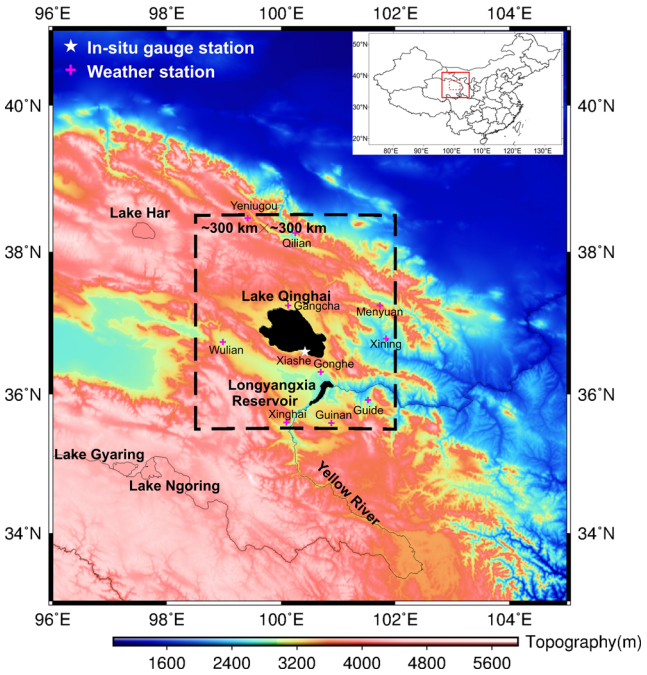

Figure 1. Location of Lake Qinghai and Longyangxia reservoir (black). The dashed square approximately corresponds to the spatial resolution of the time-variable GRACE solution (~300 km). The white stars near Lake Qinghai represent the location of the Xiashe gauge station and the red crosses represent the locations of weather stations.

input parameters (i.e. precipitation data and air temperature) of the hydrological model and *in situ* measurements to assess the performance of an LSM in the study region. Using the residuals of GRACE observations based on GRACE-derived TWS minus the contribution from an LSM and an artificial reservoir, we also examine the signal from the saturated zone, which primarily reflects changes in groundwater. The contribution of this study is to better quantify and understand large changes in lake water storage by integrating several methods. It is possible to improve our understanding of terrestrial water fluxes at a time in which large-scale climatic change is impacting freshwater resources in unpredictable ways.

2 DATA AND METHODS

2.1 Water level and volume variability in Lake Qinghai

Water-level data were obtained from observations from the Xiashe gauge station (Fig. 1) and satellite altimetric lake heights based off of LEGOS/GOHS data (http://www.legos.obs-mip.fr/soa/hydrologie/hydroweb/). Time-series of the water level, surface area and volume were obtained from a combination of the satellites Topex/Poseidon, ERS-2, GFO, Jason-1 and ENVISAT (Cretaux *et al*. 2011). The water levels in Fig. 2(a) show good agreement between *in situ* observations and satellite altimetry data, and an annual lake level increasing trend of 0.11 ± 0.03 m yr^{-1} from 2004 to 2012. To comprehensively interpret the GRACE observations shown in the dashed square of Fig. 1 (GRACE footprint size ~300 km), the influence of the dam adjacent to Lake Qinghai on water mass must be considered. Unfortunately, although Longyangxia reservoir is the largest reservoir on the Yellow River in China, historical water-level data were not archived and as a result, is not available. Alternatively, water-level records from Longyangxia reservoir are used from two data sources: (1) an *in situ* water-level measurement study that took place from 2005 to 2012 (Lu 2013), in which figure of *in situ* water-level observations in Longyangxia reservoir was shown, (2) water-level data from news reports on the Web portals (see details for the data sources in the Supporting Information), which are used to confirm validity of the first data source. The water-level records in Longyangxia reservoir show both seasonal changes and a well-pronounced peak of water storage during 2005~2006, with a water-level increasing trend of 0.85 ± 0.50 m yr^{-1} from 2005 to 2012 (Fig. 2b).

To compute GRACE-derived time-series of mass change for Lake Qinghai and compare it with the water-level signal from either the altimeter or *in situ* measurements, it is necessary to derive mass changes in the lake and reservoir based on their height–area–volume relationship. Based on water level, surface area and volume from the LEGOS/GOHS time-series, we derive a linear relationship between height, area and volume changes (Fig. 3a). Using this height–volume relationship and water level from the Xiashe gauge station, we then infer that volume changes with *in situ* water-level observations (red dots in Fig. 3c). There is excellent agreement between those results and LEGOS/GOHS-based volume time-series data. There is also a linear relationship between height and volume changes based on water level and volume data from the news reports of the Longyangxia reservoir (Fig. 3b). Due to the difficulty of discerning changes in area from news reports, the height–area relationship of the reservoir is estimated using the differences between the adjacent volumes divided by the differences between the adjacent heights (see Supporting Information). Using the height–volume relationship from Fig. 3(b), we calculate the volume changes based on *in situ* water-level measurements from Lu's (2013) work, which is consistent with the published volume results (red dots in Fig. 3d) from the Yellow River water resources bulletin (available at http://www.yellowriver.gov.cn/other/hhgb/).

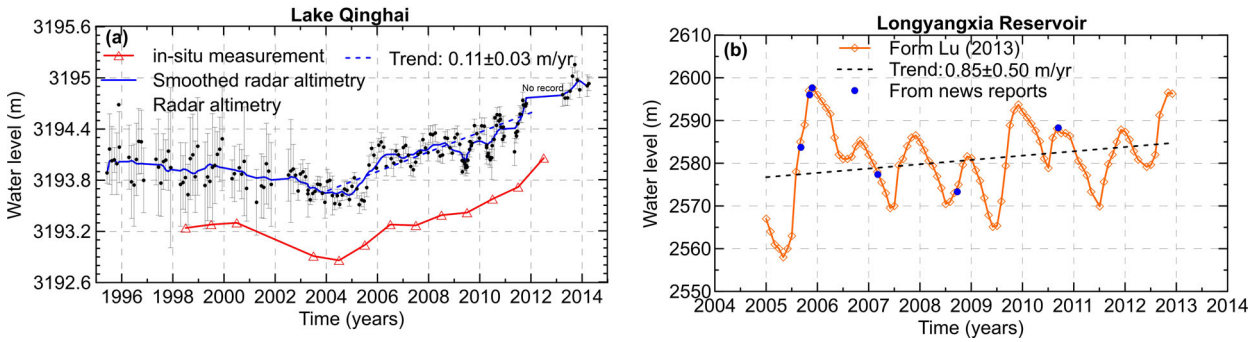

Figure 2. (a) Water level of Lake Qinghai derived from radar altimetry data and *in situ* measurements of the water level at the Xiashe station. (b) The water level in Longyangxia reservoir from two alternative data records.

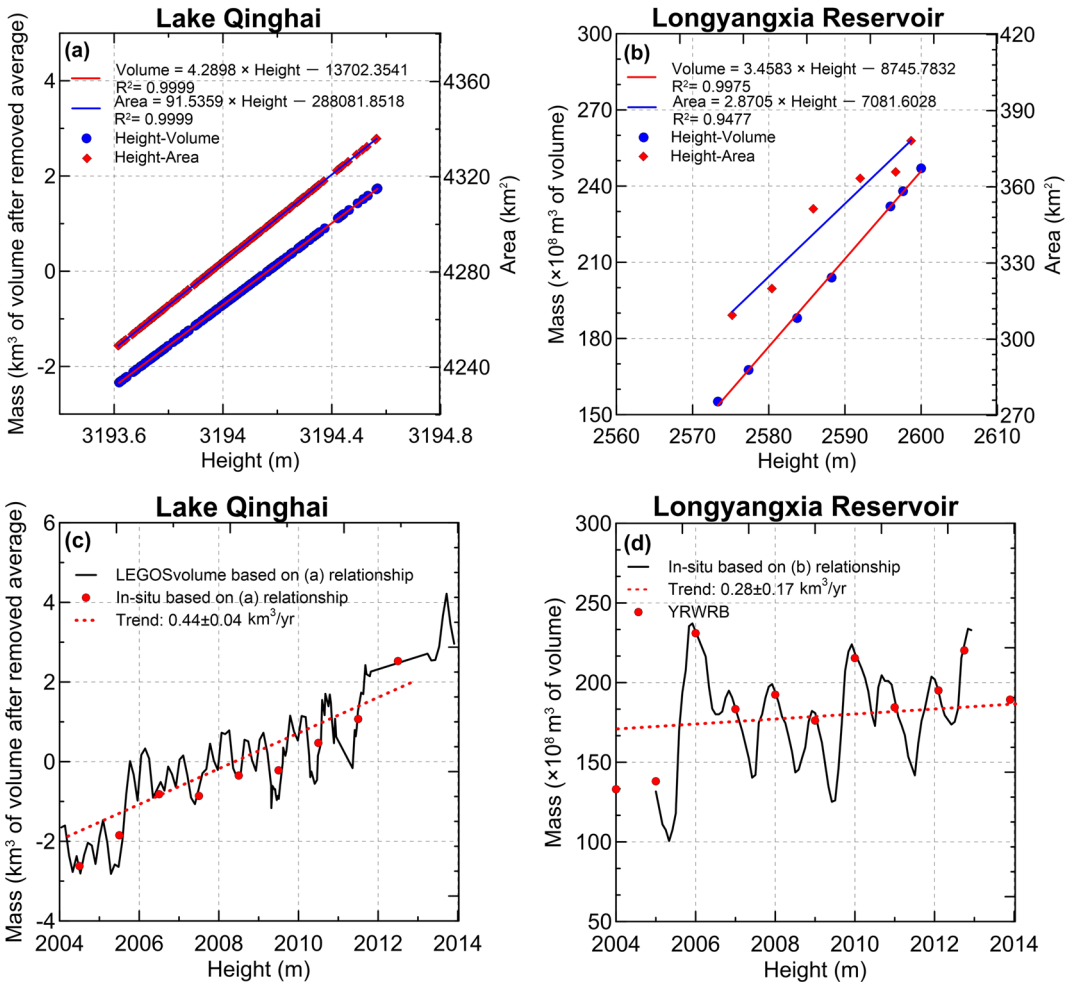

Figure 3. The linear height–area–volume relationship for (a) Lake Qinghai and (b) Longyangxia reservoir. The linear regression function is provided in the figure. Volume changes based on the linear height–volume relationship and *in situ* water-level observations for (c) Lake Qinghai and (d) Longyangxia reservoir.

2.2 GRACE data

The GRACE mission design makes it particularly useful for TWS mass change studies. GRACE was jointly launched by NASA and the German Aerospace Center (DLR) in 2002 March (Tapley *et al.* 2004). The Level-2 gravity products provide complete sets of spherical harmonic (Stokes) coefficients, typically up to the maximum degree/order $l_{\max} = 120$, averaged over monthly intervals. The Level-2 products are generated at several project-related processing centres, such as the Center for Space Research (CSR) at the University of Texas, the GeoForschungsZentrum in Potsdam, Germany and the Jet Propulsion Laboratory in California (for data sources for these three products please see the Supporting Information). The mass estimates (TWS and sea level) demonstrate very good agreement with these three products (Fu & Freymueller 2012; Wahr *et al.* 2014).

Wahr *et al.* (1998) showed that time-variable mass changes are confined to a thin layer at the Earth's surface, and discussed the methodology for converting time-variable gravity field coefficients to estimate water storage changes. The changes of vertically integrated TWS as a surface mass density (i.e. mass/area) $\Delta\sigma(\theta,\phi)$ can expand as a sum of spherical harmonics and load Love number k_l:

$$\Delta\sigma\ (\theta,\phi) = \frac{a\rho_{\text{ave}}}{3}\sum_{l=0}^{\infty}\sum_{m=0}^{l}\frac{2l+1}{1+k_l} \times \tilde{P}_{lm}(\cos\theta)\,(\Delta C_{lm}\cos(m\phi) + \Delta S_{lm}\sin(m\phi)) \quad (2)$$

Usually, the ratio $\Delta\sigma/\rho_{\text{w}}$ is defined as the EWH, where ρ_{w} is the density of water (1.0 g cm^{-3}). α is the mean radius of the Earth (α = 6371 km), ρ_{ave} is the average density of the Earth ($\rho_{\text{ave}} = 5517\,\text{kg m}^{-3}$), the $\tilde{P}_{lm}$ is normalized associated Legendre functions and the ΔC_{lm} and ΔS_{lm} are the time-variable components of the (l, m) Stokes coefficients for some month.

In this study, we use monthly sets of spherical harmonics from the GRACE Release 05 (RL05) gravity field solutions generated by CSR, spanning 2003 February to 2012 December. Each monthly GRACE field consists of a set of Stokes coefficients, C_{lm} and S_{lm}, up to degree and order (l and m) of 60. We replace the GRACE C_{20} coefficients with C_{20} coefficients inferred from satellite laser ranging (Cheng *et al.* 2013), and include the computed degree-one coefficients as calculated by Swenson *et al.* (2008). The monthly solutions have been filtered applying a Gaussian smoothing operator with an averaging radius of 250 km in order to suppress errors at high degrees (Wahr *et al.* 1998; van Dam *et al.* 2007). The Stokes coefficients from A *et al.* (2013) are used to remove the contribution of glacial isostatic adjustments (GIA). The spatial pattern of TWS, shown in Fig. 4, is obtained from the monthly GRACE mass solutions for Lake Qinghai and the surrounding regions between 2004 and 2012. A positive trend has been identified over the northeastern TP and across the entire study area (Fig. 4a). It is worth noting that GRACE observations may be very different because applied different smoothing method in study region (Yi *et al.* 2017).

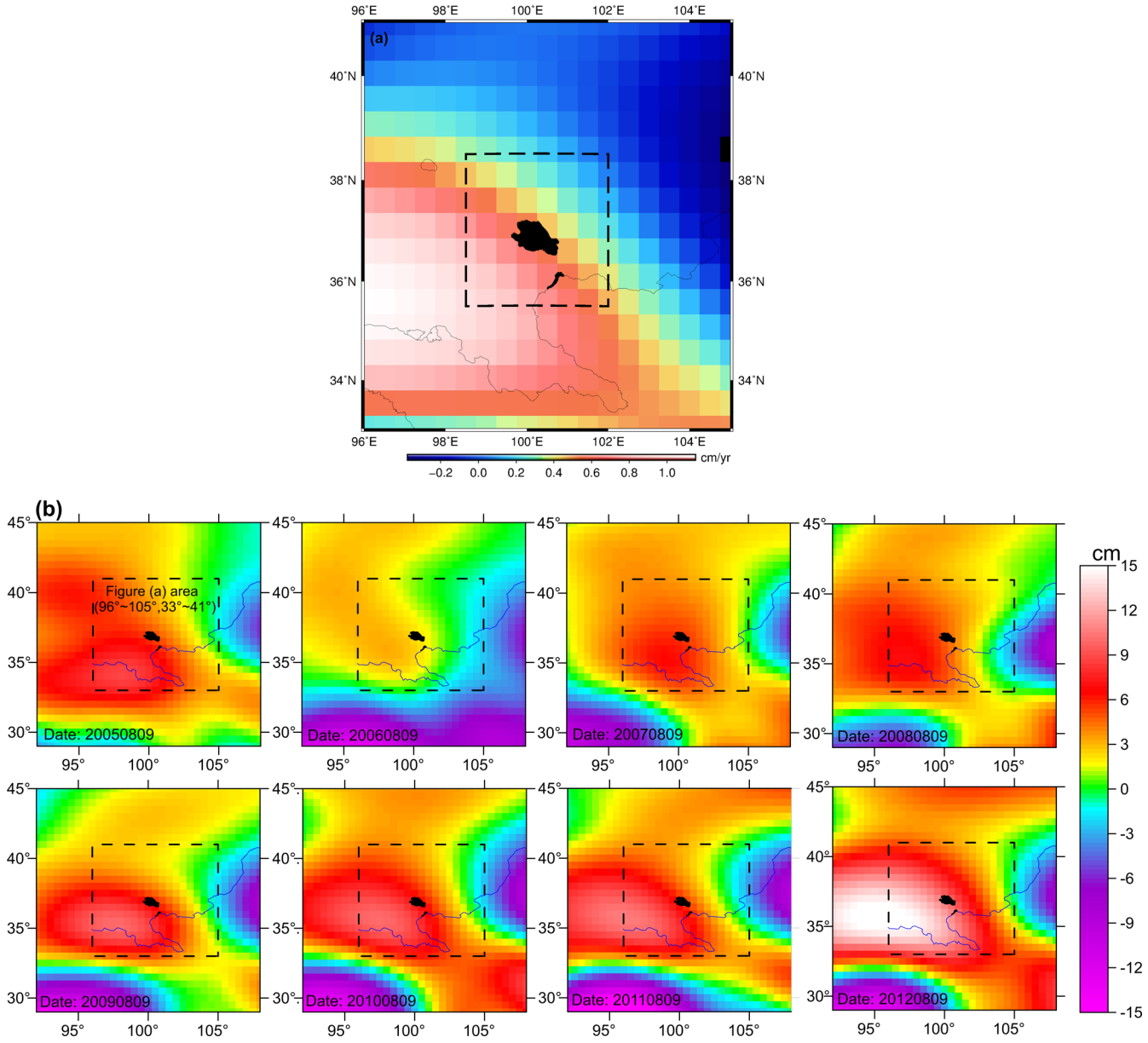

Figure 4. (a) Trends in ΔtotalWS changes in Lake Qinghai and surrounding areas derived from CSR GRACE product (RL05) after Gaussian 250 km filtered covering the period 2003–2012 in cm yr^{-1}. (b) August–September averages of TWS anomaly (after normalizing by the 2004 August–September average) in centimetres for each year of 2005–2012, from left to right starting in upper left. The black areas are locations of Lake Qinghai and Longyangxia reservoir. The dashed square in (a) approximately corresponds to the spatial resolution of GRACE (∼300 km), and the dashed square in (b) represents the scope of (a). The blue solid curve represents the Yellow River.

In this study, Gaussian smoothing method is an effective filter in suppressing noise but GRACE-derived TWS is attenuated when we using Gaussian 250 km filter. Fig. 4(b) shows August–September averages (normalized by the 2004 August–September average) in TWS for each year of 2005–2012. The TWS in the study region is found to increase by as much as 10 cm during the summer of 2005, with the maximum TWS anomaly occurring in 2012. Additionally, the monthly spatial distribution of TWS during the summers of 2005–2012 verifies the long-term increasing trend in Fig. 4(a). Besides, gravity trend in Fig. 4 implies that other effects may even be larger than that of Lake Qinghai. These facts suggest that we need to remove leakage from TWS adjacent to Lake Qinghai using LSM estimates and the method of spatial averaging kernel. To do this, first we apply an averaging kernel constructed using the weighted convolution approach described in the following section.

2.3 GRACE averaging kernel and scaling factor methods

Many applications require estimates of mass variability for specific regions, for instance, in estimating changes in water storage in a given basin. These water storage changes are generally addressed by constructing specific averaging functions optimized for an exact region, as based on the equation below (Swenson & Wahr 2002):

$$\Delta\sigma_{\text{region}} = \frac{1}{\Omega_{\text{region}}} \int \Delta\sigma\,(\theta,\phi)\,v\,(\theta,\phi)\sin\theta d\theta d\phi \qquad (3)$$

where Ω_{region} is the angular area of the region of interest, and $v(\theta, \phi)$ is the basin function constructed by covering the region with a grid of points (e.g. black areas in the dotted box of Fig. 1, the spatial resolution of grids are $0.01^\circ \times 0.01^\circ$): 1 inside the basin and 0 outside the basin. Note that the averaging kernel method uses a Gaussian averaging function at each point, and sums those averaging functions because of the finite number of harmonic degrees in the GRACE solution (e.g. $l_{\max} = 60$ for CSR solutions). In this case, the averaging kernel technique based on a weighted Gaussian convolution is used to construct monthly time-series from the GRACE Stokes coefficients (Wahr *et al*. 2014), and the generalized equation in (3) can be replaced with:

$$\Delta\sigma_{\text{region}} = \frac{1}{\Omega_{\text{region}}} \int \Delta\sigma\,(\theta, \phi)\,\bar{W}\,(\theta, \phi)\sin\theta d\theta d\phi \tag{4}$$

where $\bar{W}(\theta, \phi)$ is the weighted convolution averaging kernel:

$$\bar{W}(\theta, \phi) = \int^{W}(\alpha)\,v\left(\theta', \phi'\right) F\left(\theta', \phi'\right)\sin\theta' d\theta' d\phi' \tag{5}$$

where $W(\alpha)$ is a Gaussian smoothing function at objective region point (θ', ϕ'), which is defined as centring a function of angle α between (θ, ϕ) and (θ', ϕ'). Thus, this function underweights points near the boundary in that a point (θ, ϕ) close to boundary has points (θ', ϕ') on only one side, and then boundary points are covered by fewer Gaussian functions. To reduce underweight effect, Wahr *et al*. (2014) introduced a convolution weighting function $F(\theta', \phi')$ to accommodate non-uniform weighting of the Gaussians, that is, $F(\theta', \phi')$ near the boundary should be larger than the interior. The iterative process to find $F(\theta', \phi')$ can be found in Wahr *et al*. (2014). In this study, we use a Gaussian radius of 250 km and 20 iterations. We then apply this averaging kernel to the GRACE Stokes coefficients to obtain TWS time-series for Lake Qinghai and the surrounding regions, that is, an averaging kernel is expanded in spherical harmonics ($l_{\max} = 60$), the coefficients of those harmonics can be multiplied by the GRACE Stokes coefficients and summed to determine the region's mass variability (Swenson & Wahr 2002). In this case, the averaging kernel technique is also limited due to spatial resolution of GRACE data and remains larger than 0 for several hundred kilometres outside the region.

The result of averaging kernel is shown in Fig. 5. This kernel is reasonably uniform within their interest regions, but extends for a distance outside. Thus, the resulting time-series after applying this averaging kernel also includes contributions from outside Lake Qinghai, such as Lake Har, Lake Gyaring and Lake Ngoring (Fig. 5). Furthermore, the averaging kernel in our study is not constant for the entire Lake Qinghai area, for example, the kernel weight for Lake Qinghai and Longyangxia reservoir is 1, but the weights for the Lake Har, Lake Gyaring and Lake Ngoring are set to 0.4, 0.3 and 0.3, respectively.

For a smaller range spanned by a signal, a smaller mass is needed to generate a fixed EWH change. To recover unbiased mass estimates for this region, a scaling factor method is used to restore the amplitude-damped TWS time-series. This method suggested by Wahr *et al*. (2014) requires the construction of a set of simulated Stokes coefficients, which represents the signal from a uniformly distributed 1 m water depth change over Lake Qinghai. This gives water volumes of 1/1000 km × area change of × km^2 for Lake Qinghai (i.e. the area changes based on the linear height–area relationship in Fig. 3a). By applying our GRACE analysis procedure to these simulated Stokes coefficients, we infer the average equivalent water thickness equal to 1.34 cm for Lake Qinghai with an average area of 4298 km^2 from 2004 to 2012. The monthly GRACE estimates of water thicknesses (EWH) are then multiplied by the scaling factor 1 (m)/1.34 (cm) to obtain variations of total water thicknesses per area of Lake Qinghai. Multiplying EWH (cm) by the scaling factor [1/1000 km × area change of × km^2] (km^3)/1.34 (cm) provides the water mass change (km^3) in the lake.

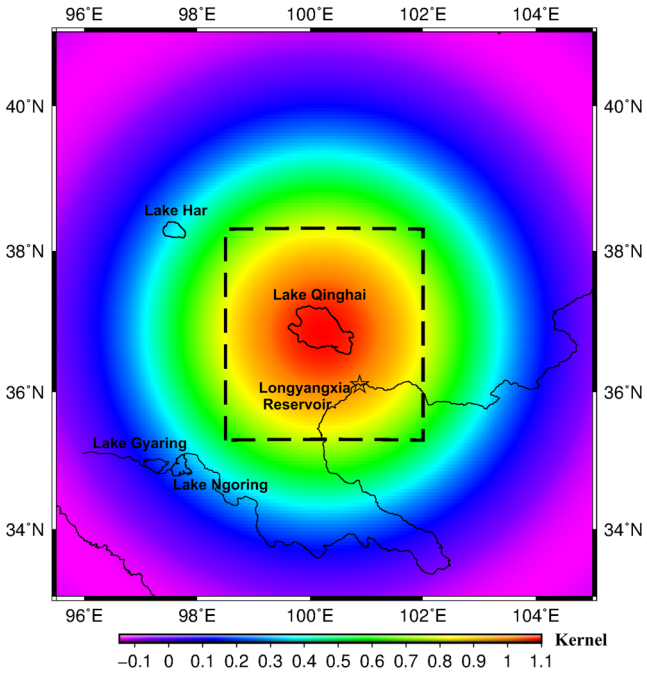

Figure 5. GRACE averaging kernels used to reveal the mass variability of Lake Qinghai. The black solid curve represents the Yellow River. The dashed square approximately corresponds to the spatial resolution of GRACE (~300 km).

2.4 Hydrological models

In general, TWS changes mainly depend on temperature variations which cause glacial melting as well as changes in precipitation and evaporation which can be simulated from global water and energy balance models (Syed *et al*. 2008). The changes in TWS are related to soil texture, snow and root depth in the case of soil water storage, which can be derived from LSM such as the Global Land Data Assimilation System (GLDAS; Rodell *et al*. 2004), the WaterGAP Global Hydrology Model (WGHM; Döll *et al*. 2003) or the Community Land Model (CLM; Oleson *et al*. 2013). However, these LSMs generate different hydrological processes, components of surface water and aquifer storage. For example, the water storage in lakes, reservoirs and wetlands can be only derived from WGHM; however, rivers and naturally occurring groundwater storage can be predicted by WGHM and CLM. Variations in TWS may also be caused by anthropogenic factors, such as water withdrawals for irrigation purposes, dam construction for power generation and navigation (Wang *et al*. 2011). These groundwater and reservoir storage changes in TWS can be measured *in situ* by making measurements of groundwater level and impounded water level. In principle, these processes can cause hydrological variations in addition to mass changes in Lake Qinghai.

Fig. 6 compares different hydrologic model simulations in the spatial averaging kernels (Fig. 5) from GLDAS/Noah, WGHM and CLM4.5 models after applying the same approach used for processing the GRACE data (i.e. a Gaussian smoothing function and an averaging kernel). While the three model simulations agree in

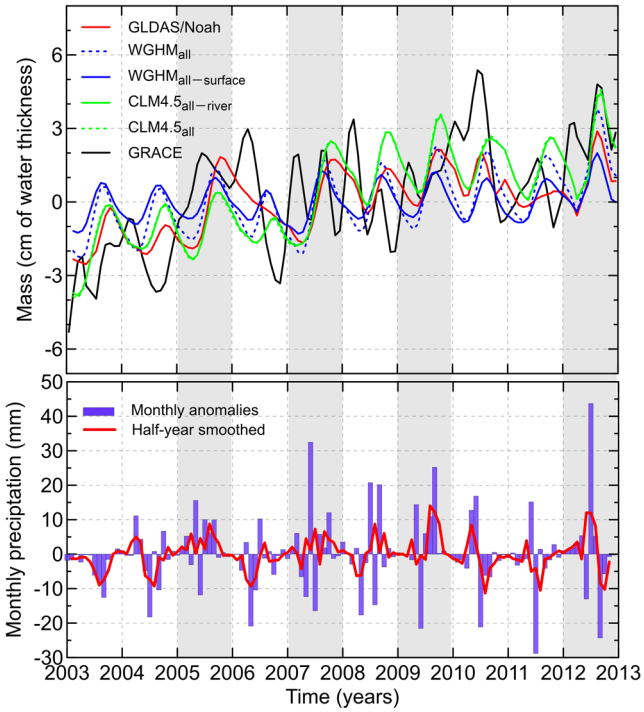

Figure 6. The above plot shows the changes in water storage from GRACE, GLDAS/Noah, WGHM and CLM4.5 models after Gaussian smoothing and applying the averaging kernel. The WGHM results include the total continental water storage (WGHMall: sum of canopy, snow, soil water, groundwater and surface water), and no surface water contributions (WGHMall–surface does not include water in rivers, lakes, reservoirs and wetlands). Similarly, the CLM4.5 results include all contributions (CLM4.5all: soil moisture, snow, canopy, groundwater and river storage), and no river contributions (CLM4.5all–river: soil moisture, snow, canopy and groundwater storage). The bottom plot shows the monthly precipitation data for weather stations located in Fig. 1 from 2003 to 2012 from China Meteorological Data Sharing Service System (CMDSSS). Areas highlighted in grey show wet years/positive water budgets in 2005, 2007, 2009 and 2012.

phases, the seasonal amplitude of the GLDAS/Noah simulations (red solid curve in Fig. 6) is much smaller than that of the WGHM_all (blue dashed curve in Fig. 6) and CLM4.5_all (green dash curve in Fig. 6) because the GLDAS/Noah model can provide values of snow (snow water equivalent) and multiple soil moisture layers (0–10, 10–40, 4–100 and 100–200 cm), but does not include anthropogenic and climate-driven groundwater changes. The CLM4.5 simulations have even larger seasonal amplitudes than the WGHM outputs due to the differences in the precipitation data set used to force the model. WGHM is forced by a combination of a Global Precipitation Climatology Centre monthly precipitation data sets from 1901 till present, which are calculated from global station data in 1.0° × 1.0° global grids (Schneider *et al*. 2014), while CLM simulations are forced by precipitation inputs in 2.5° × 2.5° global grids from the Global Precipitation Climatology Project, which are bias-corrected using merged satellite-gauge precipitation analyses.

To quantitatively evaluate which LSM fits the best in Lake Qinghai basin, and to identify which LSM solution to employ for further discussion, the relative correlation coefficients of TWS variation between GRACE and LSMs are computed. We also remove LSM-derived TWS from GRACE-observed time-series, and compute the reductions of rms (root mean squares) based on the following equation (van Dam *et al.* 2007):

$$\mathrm{rms}_{\mathrm{reduction}} = \frac{\mathrm{rms}_{\mathrm{GRACE}_i} - \mathrm{rms}_{\mathrm{GRACE}_i - \mathrm{LSM}_i}}{\mathrm{rms}_{\mathrm{GRACE}_i}} \quad (6)$$

Table 1 shows the correlation and rms reduction between GRACE and LSMs. The correlation coefficients and rms reduction between GRACE and GLDAS/Noah are 0.60 and 0.20, respectively, which are greater than the results between GRACE and other LSMs (i.e. WGHM$_{all}$, WGHM$_{all-surface}$, CLM4.5$_{all}$ and CLM4.5$_{all-river}$). This fact indicates that GLDAS/Noah is more consistent with the GRACE measurements. Moreover, TWS seasonal variations (at annual periods) and the secular trend observed from LSMs and predicted from GRACE are compared (Table 1). The LSMs and GRACE-derived trends show rise of 0.06–0.48 cm yr^{-1} for Lake Qinghai basin, which implies a continuous increase in the water storage in this region. It is clear that the LSMs (not include GLDAS) derived amplitudes are a bit larger than that derived from GRACE, and the differences of phases from LSMs are very small, but these phases are far from the GRACE result. The above discussion suggests that GRACE measurements can sense ΔtotalWS, but LSMs cannot. Thus, this will not generally be the case which the amplitude of LSMs (not include GLDAS) is greater than the GRACE data.

More importantly, we adopt GLDAS/Noah as the default model based on the following two reasons: first, our ultimate objective is to obtain an estimate of lake water variability from GRACE-derived TWS after the removal of contributions from continental water storage, not including lake and reservoir components. However, since components of TWS outputs from the CLM4.5$_{all}$ include soil moisture, snow, vegetation canopy storage, channel storage in rivers and unconfined aquifer storage and TWS outputs from the WGHM model include storage variations of water in canopy, snow, soil, groundwater, lakes, wetlands and rivers, these two models are limited to quantifying mass changes in lakes. While we can consider using the appropriate components from CLM4.5$_{all-river}$ or WGHM$_{all-surface}$, the GLDAS model is still superior at depicting the interannual variations of hydrological variables, especially when

Table 1. The correlation coefficients, rms reduction, the secular trend, annual amplitude and phase between GRACE and LSMs.

	Correlation Coefficients with GRACE (with 95 per cent confidence bounds)	rms reduction	Trend (cm yr^{-1})	Annual amplitude (cm)	Annual phase (yr)
GRACE	1	1	0.48*	0.82	0.68
GLDAS/Noah	0.60	0.20	0.27	0.70	0.21
WGHM$_{all}$	0.34	0.03	0.23	1.31	0.29
WGHM$_{all\text{-}surface}$	0.17	0.00	0.06	0.84	0.31
CLM4.5$_{all\text{-}river}$	0.45	0.04	0.47	1.17	0.21
CLM4.5$_{all}$	0.46	0.04	0.48	1.17	0.22

*GRACE-derived TWS signal (0.48 cm yr^{-1} in this study) is nearly three times smaller than estimated spatial averaging results (1.41 cm yr^{-1}) in Longyangxia Reservoir from Yi *et al*. (2017), which is mainly because of different smoothing method and specific averaging functions.

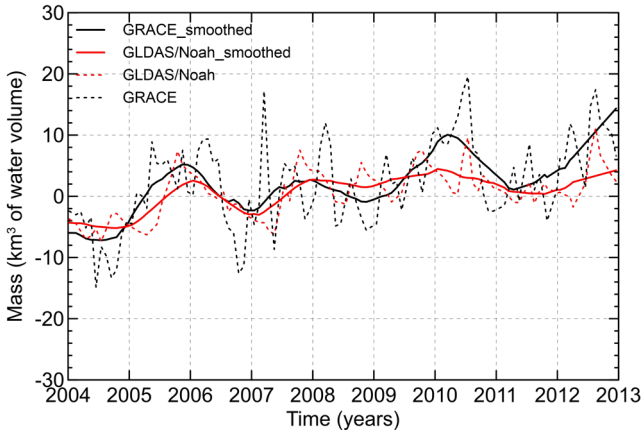

Figure 7. The mass variability estimated from GRACE data (dashed black curve for the original and solid black curve for the smoothed results), and soil moisture and snow water equivalents changes estimated from the GLDAS/Noah model (dashed red curve for the original and solid red curve for the smoothed results).

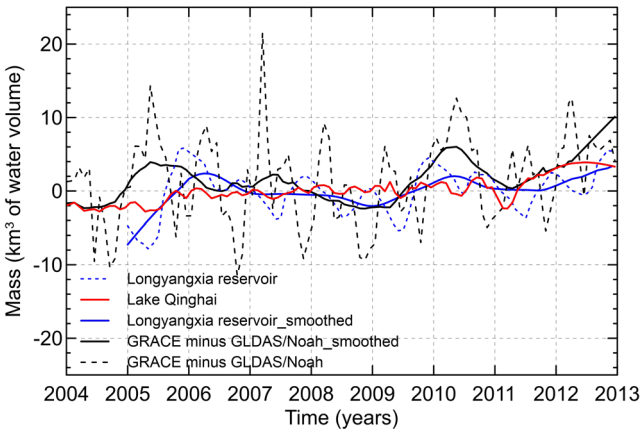

Figure 8. The mass changes estimated from GRACE-minus-GLDAS/Noah (dashed black curve for the original and solid black curve for the smoothed results). The volume changes based on the linear height–volume relationship and *in situ* water-level observations for Lake Qinghai (solid red curve) and Longyangxia reservoir (dashed blue curve for the original and solid blue curve for the smoothed results).

directly compared with water-level time-series and monthly precipitation anomalies in Lake Qinghai (Fig. 6 shows GLDAS/Noah outputs and precipitation data both exhibiting wet years/positive water budgets in 2005, 2007, 2009 and 2012). Physically, this indicates that both GLDAS modeled outputs and lake water balances are mainly driven by precipitation/evaporation changes in the basin. Therefore, GLDAS/Noah model is used to remove the contributions of soil moisture and snow water equivalents. While hydrological modeling outputs have several uncertainty problems, we have attempted to validate the performance of GLDAS/Noah outputs using the forcing input parameters (i.e. precipitation data and air temperature) from *in situ* measurements. Please see detailed discussions in Section 4 below.

3 RESULTS

3.1 Time-series estimates from GRACE and hydrological model

To compute GRACE time-series for Lake Qinghai and compare them with the water-level signal, we use the following procedure. We construct the averaging kernel for Lake Qinghai using the convolution method, as described above, and apply this averaging kernel to: (1) the destriped GRACE Stokes coefficients, and (2) the GLDAS/Noah Stokes coefficients. We derive monthly time-series of the mass variability for Lake Qinghai's 'basin function' from gridpoints. Fig. 7 compares our GRACE estimates of the TWS variability for Lake Qinghai (dashed black curves), with corresponding time-series estimated from the GLDAS/Noah model. The solid black and red curves show the results after smoothing the data with a 1-yr half-width moving window to remove seasonal and other short-period terms.

Note that both the GRACE and GLDAS/Noah model results show a continuous mass increase from 2004 to 2012 as well as a sharp change of the water storage trend that started with the onset of the rising waters in 2005. The model results seem to have no clear correlation with the onset of the wet periods in 2007, 2009 and 2012, which may result from the fact that GLDAS/Noah does not include lakes, an anthropogenic component (reservoir), or groundwater. The GRACE results, however, show an obvious mass increase which includes contributions from the adjoining lake areas due to the limited resolution of the GRACE solution. Additionally, since the sensitivity kernel (Fig. 4) is much wider than Lake Qinghai, the GRACE estimates also reflect signals well outside the Lake Qinghai area.

As described in eq. (3), the GRACE-derived ΔtotalWS changes are equally sensitive to water mass changes at all depths, (ΔSurWS, ΔSMS, ΔSnWS and ΔGWS), and include effects from adjacent regions (i.e. artificial reservoirs and other lakes). To isolate the surface water storage contributions, we subtract monthly water storage estimates from the GLDAS/Noah model results, which mainly simulate mass changes of ΔSMS and ΔSnWS at the GRACE average kernel region. After subtracting the GLDAS contributions, the GRACE-derived mass changes mainly reflect the TWS from lakes, anthropogenic contributions and groundwater. The anthropogenic impact on mass changes is investigated in the Longyangxia reservoir (blue solid curve in Fig. 8).

Fig. 8 shows GRACE-derived mass changes after removing the monthly GLDAS/Noah outputs (dashed black curve) and compares this time-series with the previously calculated volume changes based on the linear height–volume relationship and *in situ* water-level observations for Lake Qinghai and the Longyangxia reservoir. The residual signal (GRACE−GLDAS/Noah) after smoothing reveals that there is a long-term increase after 2004, or an average increasing water-level rate of 0.20 ± 0.09 m yr^{-1} (equivalent to a mass change of 0.86 ± 0.37 km^3 yr^{-1}) from 2004 to 2012 (Table 2). This demonstrates that deducting GLDAS/Noah outputs from GRACE-derived mass changes relatively has larger amplitude than Lake Qinghai, which does not merely exist in the trend rate (Table 2 shows the rate of volume is 0.44 ± 0.04 km^3 yr^{-1} from altimetric/*in situ* measurements in Lake Qinghai), but also the annual fluctuations. This difference in trends and annual fluctuations could be due to contributions from the TWS from adjacent lakes (i.e. Har, Gyaring and Ngoring) and anthropogenic factors (i.e. Longyangxia reservoir). Table 2 lists the trends for those regions.

Mass change due to the impoundment of the Longyangxia reservoir is also one of the major contributors to the GRACE-derived results. There was an abrupt increase in mass after 2005, which occurred again in 2009 and 2012, and then a slight decrease from 2006 to 2008 (Fig. 8, solid blue curve). The substantial water-level rise in wet years or decrease in dry years is closely associated with

Table 2. Water level and volume trends (with 95 per cent confidence) derived from GRACE minus GLDAS/Noah after multiplied by scaling factor, altimetry/*in situ* data and previous studies in the average kernel region during 2004–2012.

	Average area (km^2)	Water-level rate (m yr^{-1})	Kernel weight	Volume rate (km^3 yr^{-1})
GRACE[a]−GLDAS/Noah (this study)	4298 ± 28	0.20 ± 0.09[b]	1	0.86 ± 0.37
Lake Qinghai_Altimetry[c]/*In situ*	4298 ± 28	0.11 ± 0.03 (2004–2011)	1	0.44 ± 0.04
Longyangxia reservoir	326 ± 26	0.85 ± 0.50 (2005–2012)	1	0.28 ± 0.17
Lake Har[d]	607	0.17 (2003–2009)	0.4	0.04
Lake Gyaring[d]	557	0.29 (2003–2009)	0.3	0.05
Lake Ngoring[c]	628	0.66 (2004–2011)	0.3	0.12

[a]GIA contributions were removed using Stokes coefficients from A *et al*. (2013).
[b]Equivalent to water thickness (EWH) of 0.27 ± 0.12 cm yr^{-1} after mass change of 0.86 ± 0.37 km^3 yr^{-1} divided by scaling factor 4.298/1.34.
[c]Altimetric lake height for Lake Qinghai and Lake Ngoring was provided by LEGOS/GOHS.
[d]Lake area and change rate of Har and Gyaring from Song *et al*. (2014).

dramatic changes in precipitation and evaporation (Song *et al*. 2014). We also note that the mass signals inferred from GRACE (after the removal of GLDAS/Noah outputs) minus the Longyangxia reservoir probably overestimate the mass change in Lake Qinghai. This difference, which is discussed above, occurs because of leakage of the adjacent lake and groundwater signals into Lake Qinghai caused by the imperfect GRACE averaging kernel and the limit of vertical resolution.

3.2 Estimating errors and accounting for leakage

To understand leakage errors, consider an application where the goal is to use the Stokes coefficients to assess a regional water storage change. For example, suppose a surface mass average is constructed and interpreted as an estimate of water storage variability in some chosen river basin. Leakage errors are caused by gravity signals from outside the basin. For example, GRACE-derived ΔtotalWS includes soil, snow, etc. (GLDAS outputs), lakes (Lake Qinghai and others) and groundwater. The goal of this study is to estimate mass variability within a specific region (Lake Qinghai) with no contamination from regions outside. In this case, leakage is an inescapable source of error. The only way to estimate the likely impact of that error is to apply the averaging function to simulated data. This sort of problem commonly arises in time-series analysis. As described above, an averaging function should usually be smoother than the basin function to provide an accurate estimate.

In this paper, we use spatial averaging kernels to isolate the gravity signal from individual regions (i.e. Lake Qinghai), while simultaneously minimizing the effects of GRACE observational errors and of surrounding glacial and hydrological signals. Although the mass trend computed using the GRACE sensitivity kernel is clearly positive from 2004 to 2012, the residual signal (GRACE−GLDAS−Reservoir) also likely reflects mass leakage from areas surrounding the lake. In fact, previous studies have shown accelerated expansion of lakes on the TP in the 2000s (e.g. Zhang *et al*. 2013; Song *et al*. 2014, 2015). The continued growth trend that appears over Lake Qinghai from the GRACE-derived model presumably includes leakage from the adjacent large-scale lakes. To estimate measurement error from GRACE and quantitatively evaluate leakage effects from land water storage adjacent to Lake Qinghai, we compare the increasing rates of lake volume from the GRACE-derived solution and radar altimetry (Table 2) based on a variable lake area (× km^2). It is also important to determine the kernel weight for all lakes in the GRACE averaging kernel region (Fig. 4).

To obtain mass rates for each lake, we use the results of Song *et al*. (2014) for lake level and area of Lake Har and Lake Gyaring. Song *et al*. (2014) also showed a change rate of 0.11 m yr^{-1} associated with the accelerated expansion of Lake Qinghai, which is in good agreement with our results (Table 2). Results also agree on the calculated average area, as our results indicate an area of 4298 ± 28 km^2 from 2004 to 2012, while previous results found areas of 4318 km^2 in 2008 from Zhang *et al*. (2011b) and 4307.89 km^2 from Song *et al*. (2014). The most recent studies have suggested that Lake Qinghai is more than 4400 km^2 as measured in 2015, growth that has resulted from the water level rising (http://www.gov.cn/xinwen/2016–05/18/content_5074478.htm). In fact, this volume difference is expected based on previous studies that estimated a growth rate of 0.11 m yr^{-1} associated with accelerated lake expansion, and represents less than a ∼0.01 km^3 expected difference from the latest survey area (4400 km^2). Table 2 lists the trends in mass change of these large lakes in the averaging kernel region. The statistical results show the GRACE-derived mass residual trend (the volume rate based on GRACE−GLDAS/Noah−reservoir−Lake Qinghai is 0.14 ± 0.41 km^3 yr^{-1} under the kernel weight equal to 1), which is similar to the volume trend of adjacent lakes as measured via radar altimetry from 2003 to 2009 (the volume rate is 0.21 km^3 yr^{-1} based on Lake Har + Lake Gyaring + Lake Ngoring using the kernel weights 0.4, 0.3 and 0.3, respectively).

However, leakage errors can also come from time-variable mass anomalies below the basin. Signals below the basin could come from underlying solid Earth (i.e. GIA and tectonic processes) or the saturated zone (i.e. groundwater), and cannot be separated from the GRACE signal even after GLDAS outputs are removed. Details of the analysis of the mass anomalies below the basin are provided in Section 4.

4 DISCUSSIONS

4.1 The abrupt water storage change from 2004 to 2006

According to the records from the Xiashe hydrological station provided by the Bureau of Hydrology and Water Resources in Qinghai Province, the water level of Lake Qinghai experienced a steady decrease from 3196.95 m in 1959 to 3193.20 m in 2004, but increased to 3194.09 m from 2004 to 2009 with a maximum rate of 0.68 m from 2005 April to October (Zhang *et al*. 2011b). Other studies have also shown large water level rises in many lakes in the central and northeastern TP in this time period (Song *et al*. 2014; Wang *et al*. 2016).

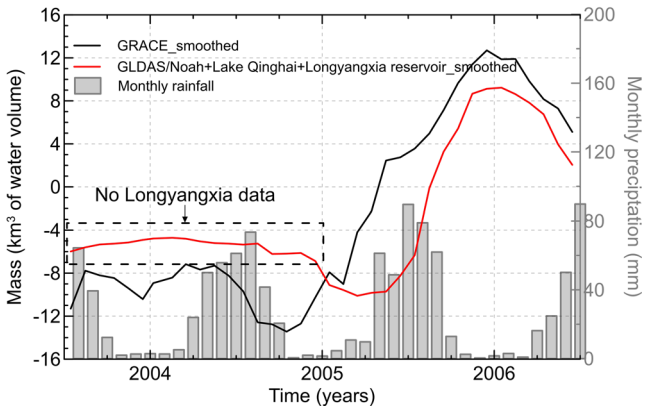

Figure 9. Temporal changes in water storage and monthly precipitation data (rainfall amount averaged from 10 weather stations located in Fig. 1) from 2004 to 2006, including GRACE-derived mass change (solid black curve), sum of mass change (solid red curve) observed from radar altimetry, contributions from the GLDAS/Noah and the Longyangxia reservoir (*in situ* water-level measurement only during 2005–2012).

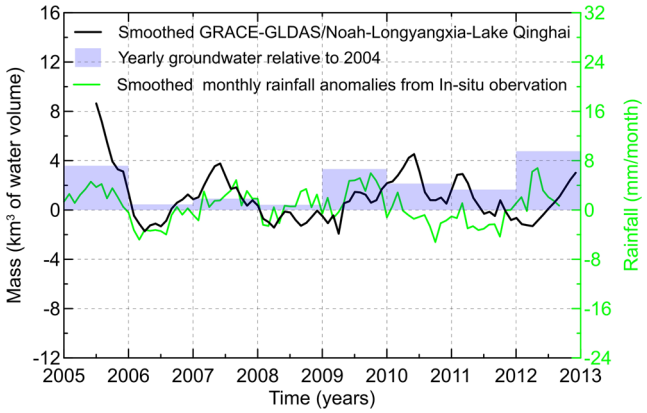

Figure 10. Comparison of the GRACE-derived GWS anomalies and yearly groundwater mass changes from QHWRB during 2005–2012. *In situ* rainfall anomalies (solid green curve) are averaged from 10 weather stations located in Fig. 1.

In this study, GRACE-derived results also indicate a notable decrease in water levels in 2004 followed by a significant increase from 2005 to 2006 (black solid curve in Fig. 9). During 2005 and 2006, observed average rainfall amplitudes (i.e. red crosses located in Fig. 1 and data from CMDSSS) suggest that the northeastern TP experienced major wet periods in 2005 with rainfall anomalies larger than the previous two years. This result confirms that the abrupt TWS shift in the study region is primarily associated with changes in the water balance controlled by runoff, evapotranspiration and precipitation due to rapid climate changes.

To capture the potentially equally rapid response of the hydrological signal variables during this period, we compare GRACE anomalies with hydrological model results for both Longyangxia reservoir and Lake Qinghai (Fig. 9). The results show that the abrupt TWS shift in 2005 is due to almost equal contributions from snow water storage, soil moisture storage and surface water reservoir storage (i.e. lakes and artificial reservoirs). While the phase of the change in mass since 2005 in the Longyangxia reservoir does not exactly correspond to other water storage components, this difference can be explained by the fact that the reservoir is controlled by both climatic and anthropogenic factors. Generally, water levels are controlled by the dam on an annual scale to gain the most power generation benefits, maintain adequate water allotment for downstream, and keep at a reasonably low water level to prepare for flood control during the monsoon season.

Clearly, GRACE-derived mass fluctuations reflect variations in the total water balance of the lake and its surrounding areas due to the limited resolution of the GRACE solutions ($l_{max} = 60$) and the Gaussian filtering, which might cause leakage effects. Therefore, the increased rate of the GRACE-derived mass change is greater than the water level rise. This result confirms that the spatial averaging kernels can isolate the gravity signal of individual regions and minimize the effects of GRACE observational errors. However, there is still a need to use complementary models or *in situ* observations to eliminate the influence of hydrological, GIA and tectonic processes (e.g. crustal uplift and thickening, see Section 4.2).

4.2 GWS, GIA and tectonic processes

Another important component of water storage estimates from GRACE is the groundwater contribution to TWS. Groundwater processes act as a low-pass filter for precipitation, allowing longer term signals associated with climate change to appear in the groundwater record. Groundwater signals are also particularly susceptible to anthropogenic changes, for example, aquifer pumping to obtain water for agricultural and urban use, and groundwater infiltration from irrigation. Because few large-scale LSMs include groundwater storage, and fewer still include anthropogenic effects, contributions such as these cannot be extracted from models. Thus, time-variable satellite gravity measurements offer a means of monitoring this variability. GWS is estimated in this study by GRACE-derived mass change after removing the mass contributions from GLDAS/Noah, Longyangxia reservoir and Lake Qinghai (Fig. 10).

In order to validate the results in this study, we compare our GRACE-based GWS estimate with yearly groundwater measurements of whole Qinghai province from the Qinghai Water Resources Bulletin, 2005–2012 (QHWRB, available at: http://www.qhsl.gov.cn/NewShow.aspx?id=46420) and with field measurement data of precipitation anomalies (e.g. *in situ* rainfall amount from weather stations from CMDSSS). Fig. 10 shows that the GRACE-based estimate (solid black curve) is generally consistent with the yearly groundwater mass changes (blue bar) from QHWRB during 2005–2012, which shows a GWS increase in 2005 that slows down from 2006 to the end of 2008, and then increases again after 2009. These groundwater fluctuations are mainly induced by climatic-scale precipitation recharge (solid green curve) in the study region.

Besides the significant mass changes discussed above, there is also a complicated signal in the GRACE-derived results induced by GIA and tectonic vertical movements in the TP. In this study, we have removed possible effects of GIA using the Stokes coefficients computed by A *et al.* (2013), which are based on the ICE5G ice history and the VM2 viscosity profile (Peltier 2004). The contribution of GIA is about 1.7–1.9 mm yr^{-1} in the spatial averaging kernels. Zhang & Jin (2013) showed that the uplift rates of GIA range from 1 to 2 mm yr^{-1} in most parts of the TP. The GIA effects computed by A *et al.* (2013) (assuming a compressible Earth and considering polar wander feedback, degree-one terms and a self-consistent ocean) are in good agreement with the results of Zhang & Jin (2013) based on four global GIA models and four regional models. The last ones estimate the GIA uplift rates for various ice sheet and viscoelastic Earth models. Although the predicted effects from these models are small (<2 mm yr^{-1} in the TP), a large uncertainty still exists because the volume of the late Pleistocene ice sheet is highly

speculative. Therefore, the uncertainties of GRACE-derived results in Lake Qinghai include error from the GIA correction.

The TP is also influenced by various tectonic processes, leading to an ongoing uplift, large crustal deformation and thickening and active seismicity due to its collision with the Indian plate (Tapponnier *et al*. 2001). At the front of the collision zone, South Tibet is significantly affected by all these processes (Yi *et al*. 2016a). Previous studies (e.g. Sun *et al*. 2009; Chen *et al*. 2016) have shown a regional gravity change of -0.2 to -0.6 ± 0.05 and $-0.66 \pm 0.49\ \mu\text{Gal yr}^{-1}$ associated with ground uplift and crustal thickening, respectively, in South Tibet. Therefore, the long-term gravity change related to tectonic movements likely contributes negatively to the current GRACE-derived mass increase determined in this study. However, most studies have focused on gravity changes and deformations in the HMA, while only a few have systematically investigated the entire plateau, especially the northeast. Gravity change in eastern Tibet was found to be $0.32 \pm 0.08\ \mu\text{Gal yr}^{-1}$ during 2003–2014 by Yi *et al*. (2016b) after removing signals from Qinghai Lake, soil moisture and glacier melt. Their results imply that tectonic process due to a crustal flow may cause a positive gravity trend, but they also point out that uncertainty in the gravity trend greatly impedes a refined understanding of the interior dynamics. In this study, we ignore the tectonic processes impacts on gravity change in TP, and assume the long-term gravity change revealed by GRACE data is mainly because of the mass increase. Thus, the error of Lake Qinghai mass estimate includes effect of tectonic processes.

4.3 Assessing the performance of GLDAS/Noah

Various studies try to use LSM outputs to improve the vertical resolution of GRACE. In this study, the GLDAS/Noah model is used to estimate the contributions of soil moisture and snow water equivalent in TWS compartments to separate the GRACE-derived TWS for the purpose of quantifying mass change in Lake Qinghai. Thus, uncertainty in our estimated results from GRACE is largely affected by the amount of uncertainty from the GLDAS/Noah model outputs. Because the GLDAS model does not simulate groundwater and river channel storages (Rodell *et al*. 2004) and is not calibrated against field measurements, water storage estimates predicted by the GLDAS/Noah are probably overestimated or underestimated. To attempt and minimize LSM end-product uncertainty, the model forcing inputs (e.g. precipitation and temperature) can be compared with *in situ* measurements, to help assess and improve those models.

In this paper, we investigate whether there are significant observed differences in spatial distribution and in the time-series between the GLDAS/Noah input forcing data and available field measurements. The Nash–Sutcliffe efficiency (NSE) coefficient calculated as follows is used to evaluate the degree of statistical agreement between GLDAS/Noah results and *in situ* measurements.

$$\text{NSE} = 1 - \frac{\sum_{i=1}^{n} (\text{in\_situ}_i - \text{GLDAS}_i)^2}{\sum_{i=1}^{n} \left(\text{in\_situ}_i - \text{in\_situ}_{\text{average}}\right)^2} \tag{7}$$

Where in_situ_i is the *in situ* observed data, GLDAS_i is the forcing inputs of GLDAS/Noah, n is number of measurements and $\text{in\_situ}_{\text{average}}$ is the average of in_situ_i (from 2003 January to 2012 December). Ideally, the optimal value for the NSE indicating perfect agreement is 1.0.

Fig. 11 shows the monthly average rainfall observed from the weather stations (Fig. 11a) and extracted from the GLDAS forcing rainfall data (Fig. 11b) in the northeast TP. Note that the *in situ* rainfall and air temperature data set are calculated from 2472 stations into $0.5^\circ \times 0.5^\circ$ grids, with horizontal resolution higher than that of GLDAS forcing inputs ($1.0^\circ \times 1.0^\circ$). Over the study region (black dotted box), the amplitude of monthly rainfall from *in situ* data is approximately 40 mm month^{-1}, which is larger than rainfall from GLDAS estimated at approximately 25 mm month^{-1}. This comparison shows that the GLDAS model may underestimate the true TWS signal in this area. The rainfall time-series for the selected basins are displayed in Fig. 11(c). The correspondence between the *in situ* and GLDAS is also reflected in the NSE coefficient (0.82). Fig. 11(c) shows an excellent agreement with phases between the two types of data, but the amplitude is different in the summer of each year.

Fig. 12 shows the average monthly air temperature from *in situ* observations (Fig. 12a) and GLDAS forcing rainfall data (Fig. 12b) in the northeast TP. There is clearly excellent agreement with air temperature observations over the study region, as can be seen in Fig. 12(c), which shows good consistency between the amplitudes and phases of the air temperature data from weather stations and GLDAS model, reaching a high NSE value of 0.95.

Analysis of rainfall and temperature data suggests that the differences in forcing precipitation are likely to be the main cause for GLDAS underestimation of the actual storage changes in summer months. Precipitation amount and timing have an important impact on surface water storage. In response to the anomalously large precipitation amounts in 2005 (Fig. 11c), the GRACE time-series shows TWS increase (Fig. 9). We also find that precipitation in this region exhibits strong interannual variability, with high precipitation around 2007 and 2012 again. In fact, LSMs are the best available tools for making long-range predictions of both natural and anthropogenic TWS variability. Differences in TWS between GRACE and GLDAS are attributed in part to differences in precipitation input. Although not demonstrated in this study, the use of corrected LSM outputs based on *in situ* data will provide more accurate results when these outputs are used to refine the vertical and horizontal resolutions of GRACE, which will in turn reduce the uncertainty in GRACE-based estimates of mass changes from lakes.

5 CONCLUSIONS

Lake Qinghai plays a crucial role in maintaining the ecological health and water balance of the great river basins in the TP. Its behaviour reflects water dynamics associated with long-term trends in regional and global climate change. In this study, we develop a simple framework to estimate water storage variations in the Lake Qinghai region while simultaneously minimizing the effects resulting from uncertainties of GRACE observations and other factors related to surrounding hydrological signals. The regional mass increase in Lake Qinghai is estimated from GRACE-derived TWS, hydrological model and reservoir water-level data from 2004 to 2012. The obtained results are compared with different data sources to improve the horizontal and vertical resolutions of GRACE data. The main conclusions are as follows.

(1) We select three LSMs (GLDAS/Noah, WGHM and CLM4.5) to quantitatively assess which LSM fits the best in Lake Qinghai basin. Our findings indicate that the GLDAS/Noah hydrology model is a relatively optimal hydrological model. The GLDAS/Noah model depicts the interannual variations of hydrological variables better than the other two models tested (WGHM and CLM4.5) when the correlation coefficients and rms reduction of TWS variation between GRACE and LSMs are compared. We also find that the differences

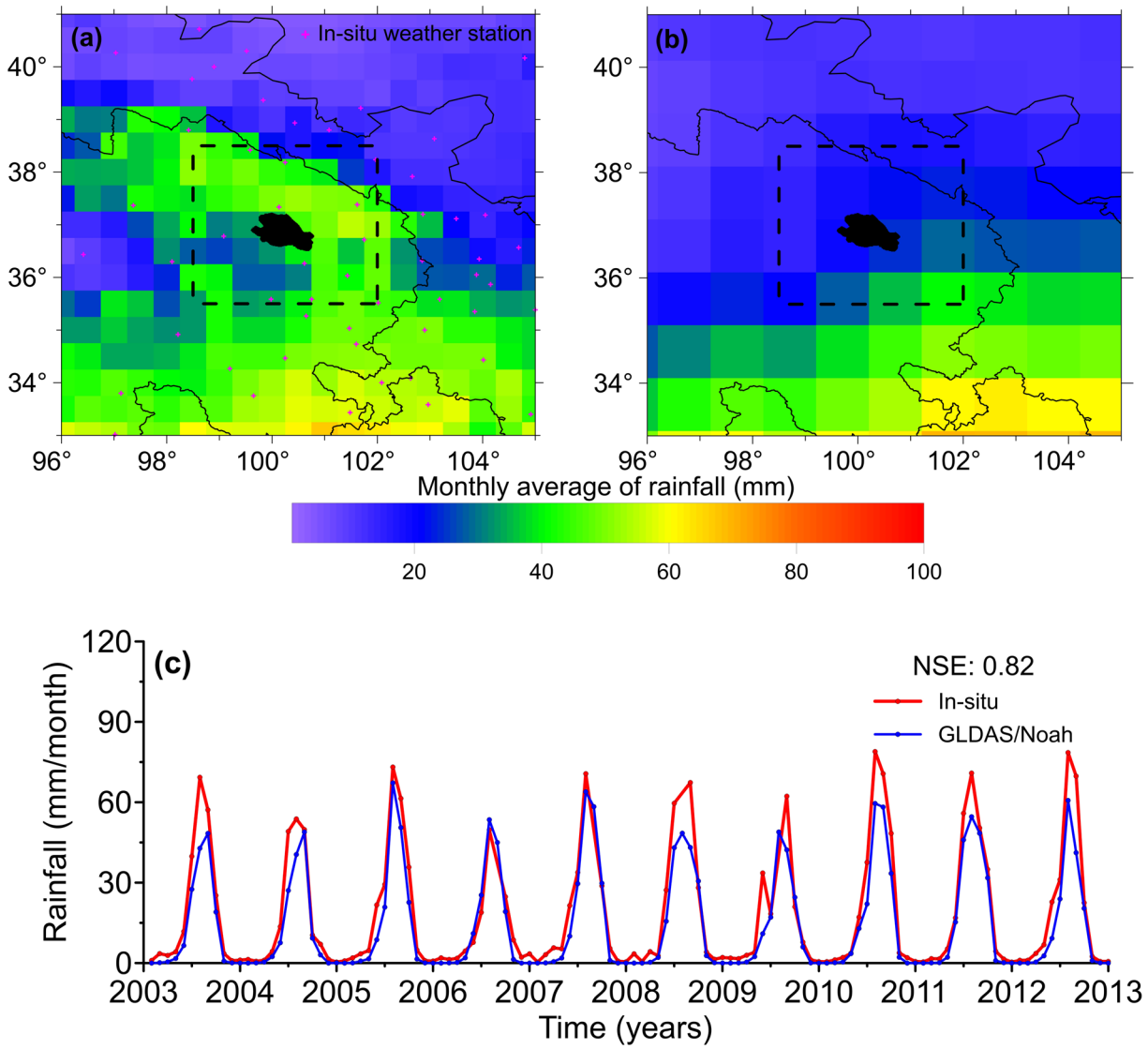

Figure 11. Average monthly rainfall (in mm month^{-1}) from *in situ* (a) and GLDAS forcing data (b) in the northeast TP during the period 2003 January–2012 December, and (c) time-series showing the temporal variations in monthly rainfall for the selected basin (black dotted box in Fig. 11a).

in precipitation between *in situ* observations and GLDAS forcing inputs are likely to be the main cause for GLDAS underestimating the actual storage changes in summer months. To improve the performance of a wide range of LSMs, we suggest finding sufficient forcing parameters via *in situ* measurements, which allows us to accurately calculate the simulations when we combine GRACE and LSMs to monitor one of the components from TWS.

(2) After subtracting supplementary effects (e.g. soil moisture and snow) predicted by GLDAS/Noah, the mass increase rate of the GRACE-derived EWH is calculated to be 0.27 ± 0.12 cm yr^{-1} from 2004 to 2012, which is equivalent to the volume 0.86 ± 0.37 km^3 yr^{-1} and higher than the result derived from radar altimetry and *in situ* estimates of the mass increase rate in Lake Qinghai (a volume of 0.44 km^3 yr^{-1} based on the water-level rate of 0.11 m yr^{-1}). The estimates in this study reflect the total mass signals from surface and subsurface water storage, including lakes, reservoir and groundwater.

(3) We demonstrate that the abrupt changes in water storage from 2004 to 2006 and the long-term storage increase from 2005 are mainly due to the fast expansion of Lake Qinghai, the impoundment of Longyangxia reservoir, and other changes in water storage signals simulated by GLDAS/Noah. When comparing with available observations in Longyangxia reservoir, we observe that the phases of mass change since 2005 do not exactly correspond to other water storage components, because Longyangxia reservoir is controlled by both climatic and anthropogenic factors.

(4) The difference between GRACE estimates and altimetry data indicates that the residual signal (GRACE−GLDAS/Noah−reservoir−Lake Qinghai) likely reflects the mass leakage from the regions surrounding the lake, or the hydrology model does not include all contributions due to the limited spatial resolution of GRACE. We quantitatively evaluate the leakage from the adjacent lakes (i.e. Har, Gyaring and Ngoring) and groundwater contributions. The statistical results show that the GRACE-derived mass trend is close to the sum of the volume trend from radar altimetry and *in situ* measurements, and the annual fluctuations of residual signal closely resemble to the yearly groundwater mass changes from QHWRB during 2005–2012.

Finally, this study demonstrates whether water storage variations in individual regions (i.e. Lake Qinghai far smaller than the spatial

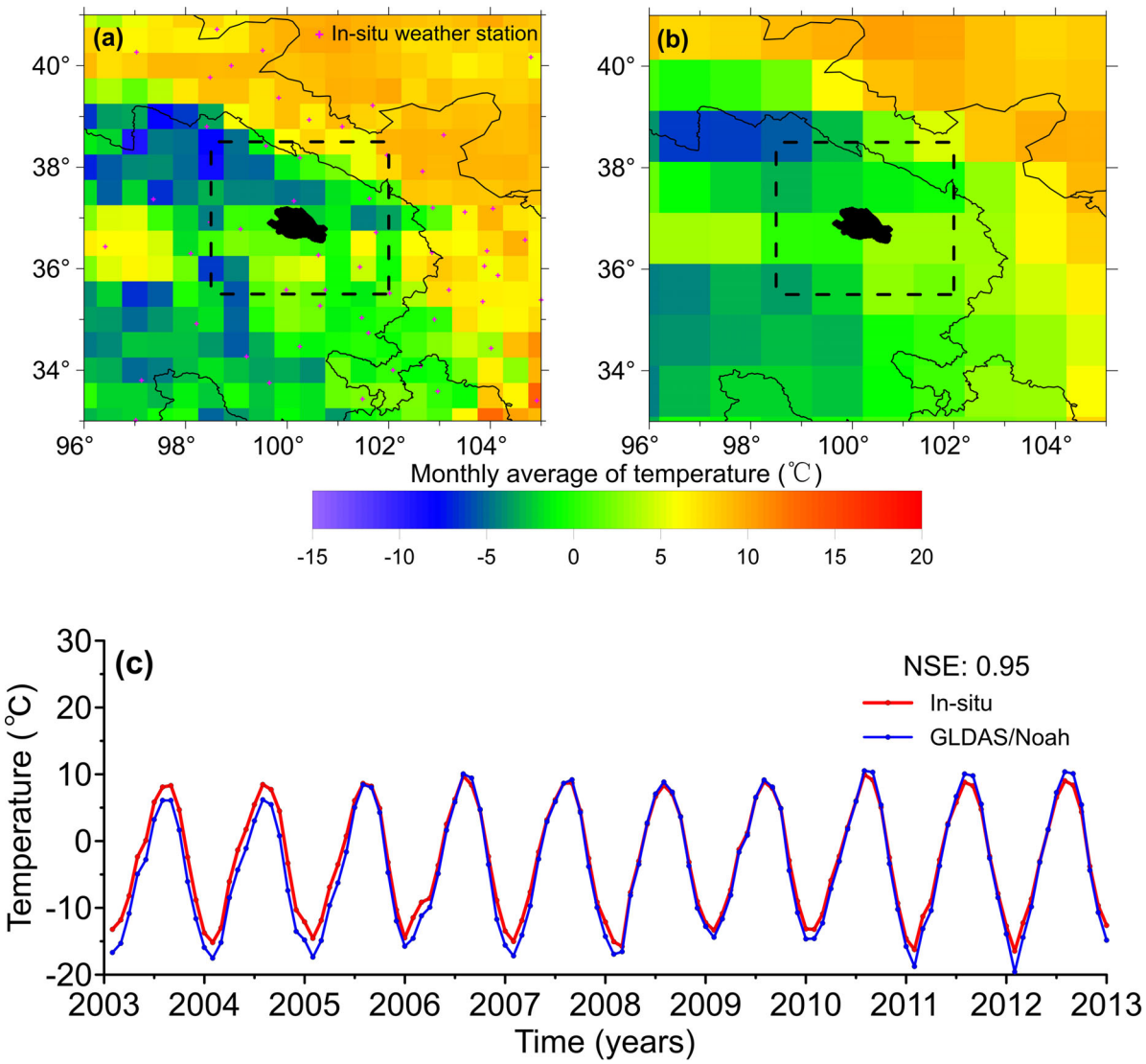

Figure 12. Average monthly air temperature (in °C) from *in situ* (a) and GLDAS forcing data (b) in the northeast TP during the period 2003 January–2012 December and (c) time-series showing the temporal variations in monthly air temperature for the selected basin (black dotted box in Fig. 12a).

resolution of GRACE) can be monitored by GRACE, while we simultaneously minimize the effects resulting from uncertainties of GRACE observations and other factors related to the surrounding TWS signals. We should clarify that the uncertainty in the TWS trend of Lake Qinghai is greatly affected by the error of each contributors to the GRACE observation including leakage error, GIA and tectonic processes error, uncertainty of GLDAS/Noah, and effect of GWS. These contributing factors probably limit the accuracy in the estimation of TWS in small spatial coverage.

ACKNOWLEDGEMENTS

We thank Editor Prof. Kosuke Heki and two anonymous reviewers for their detailed, helpful and insightful comments. The authors gratefully appreciate the Laboratoire d'Etudes en Geodesie et Oceanographie Spatiales, Equipe Geodesie, Oceanographie, et Hydrologie Spatiales (LEGOS/GOHS) and the Hydrology and Water Resources Survey Bureau of Qinghai province for the water-level data of Lake Qinghai. We also thank the Center of Space Research (CSR) teams for their online accessible GRACE solutions and the GLDAS/Noah model data provided by the NASA Goddard Earth Sciences Data and Information Services Center (GES DISC). This work was initiated while LW was visiting Prof. John Wahr at the Department of Physics, University of Colorado at Boulder. We are grateful to Prof. John Wahr for providing CLM4.5 Stokes coefficients produced by National Center for Atmospheric Research (NCAR). We also appreciate Li Chen for his valuable suggestions on revising and polishing this paper. This work is supported by the National Natural Science Foundation of China (NSFC) (grant nos. 41504065, 41574070 and 41604060), China Postdoctoral Science Foundation funded project (grant no. 2014T70753) and the Fundamental Research Funds for the Central Universities, China University of Geosciences (Wuhan).

REFERENCES

A, G., Wahr, J. & Zhong, S., 2013. Computations of the viscoelastic response of a 3-D compressible earth to surface loading: an application to glacial isostatic adjustment in Antarctica and Canada, *Geophys. J. Int.*, **192,** 557–572.

Becker, M., LLovel, W., Cazenave, A., Güntner, A. & Cretaux, J.F., 2010. Recent hydrological behavior of the East African great lakes region

inferred from GRACE, satellite altimetry and rainfall observations, *C. R. Geosci.,* **342,** 223–233.
Chen, S., Liu, M., Xing, L., Xu, W., Wang, W., Zhu, Y. & Li, H., 2016. Gravity increase before the 2015 Mw7.8 Nepal earthquake, *Geophys. Res. Lett.,* **43,** 111–117.
Cheng, M.K., Tapley, B.D. & Ries, J.C., 2013. Deceleration in the earth's oblateness, *J. geophys. Res.,* **118,** 1–8.
Cretaux, J.F. *et al.*, 2011. SOLS: a lake database to monitor in the Near Real Time water level and storage variations from remote sensing data, *Adv. Space Res.,* **47,** 1497–1507.
Döll, P., Kaspar, F. & Lehner, B., 2003. A global hydrological model for deriving water availability indicators: model tuning and validation, *J. Hydrol.,* **270,** 105–134.
Feng, W., Zhong, M., Lemoine, J.M., Biancale, R., Hsu, H.T. & Xia, J., 2013. Evaluation of groundwater depletion in North China using the Gravity Recovery and Climate Experiment (GRACE) data and ground-based measurements, *Water Resour. Res.,* **49,** 2110–2118.
Fu, Y. & Freymueller, J.T., 2012. Seasonal and long-term vertical deformation in the Nepal Himalaya constrained by GPS and GRACE measurements, *J. geophys. Res.,* **117,** B03407, doi:10.1029/2011JB008925.
Gardner, A.S. *et al.*, 2013. A reconciled estimate of glacier contributions to sea level rise: 2003 to 2009, *Science,* **340**(6134), 852–857.
Huang, L., Liu, J., Shao, Q. & Liu, R., 2011. Changing inland lakes responding to climate warming in Northeastern Tibetan Plateau, *Clim. Change,* **109**(3–4), 479–502.
Immerzeel, W.W., van Beek, L.P.H. & Bierkens, M.F.P., 2010. Climate change will affect the Asian water towers, *Science,* **328**(5984), 1382–1385.
Jacob, T., Wahr, J., Pfeffer, W.T. & Swenson, S., 2012. Recent contributions of glaciers and ice caps to sea level rise, *Nature,* **482**(7386), 514–518.
Kang, S., Chen, F., Gao, T., Zhang, Y., Yang, W., Yu, W. & Yao, T., 2009. Early onset of rainy season suppresses glacier melt: a case study on Zhadang glacier, Tibetan Plateau, *J. Glaciol.,* **55**(192), 755–758.
Landerer, F.W. & Swenson, S.C., 2012. Accuracy of scaled grace terrestrial water storage estimates, *Water Resour. Res*., **48,** 4531, doi:10.1029/2011WR011453.
Li, X. *et al.*, 2008. Cryospheric change in China, *Global Planet. Change,* **62**(3), 210–218.
Liao, J., Shen, G. & Li, Y., 2012. Lake variations in response to climate change in the Tibetan Plateau in the past 40 years, *Int. J. Digital Earth,* **6**(6), 534–549.
Liu, J., Wang, S., Yu, S., Yang, D. & Zhang, L., 2009. Climate warming and growth of high-elevation inland lakes on the Tibetan Plateau, *Global Planet. Change,* **67**(3–4), 209–217.
Long, D. *et al.*, 2015. Deriving scaling factors using a global hydrological model to restore grace total water storage changes for china's yangtze river basin, *Remote Sens. Environ.,* **168,** 177–193.
Lu, C.X., Yu, G. & Xie, G.D., 2005. Tibetan plateau serves as a water tower, in *Geoscience and Remote Sensing Symposium, IGARSS '05, Proceedings, 2005 IEEE International,* Vol. **5,** pp. 3120–3123, doi:10.1109/IGARSS.2005.1526498.
Lu, Y., 2013. Analysis of transfusion in G4 cleavage belt of the Longyangxia Reservoir with its water level higher than 2594 m, *QingHai Hydroelectr. Gener.,* **4,** 51–54 (in Chinese).
Matsuo, K. & Heki, K., 2010. Time-variable ice loss in Asian high mountains from satellite gravimetry, *Earth planet. Sci. Lett.,* **290,** 30–36.
Oleson, K.W. *et al.*, 2013. *Technical Description of Version 4.5 of the Community Land Model (CLM), NCAR Tech. Note NCAR/TN-5031STR*. 434 pp, National Center for Atmospheric Research, Boulder, Colorado.
Peltier, W.R., 2004. Global glacial isostasy and the surface of the ice-age earth: the ice-5 G (VM2) model and GRACE, *Annu. Rev. Earth planet. Sci.,* **32,** 111–149.
Phan, V.H., Lindenbergh, R. & Menenti, M., 2012. ICESat derived elevation changes of Tibetan lakes between 2003 and 2009, *Int. J. Appl. Earth Obs. Geoinform.,* **17,** 12–22.
Qiu, J., 2008. China: the third pole, *Nat. News,* **454**(7203), 393–396.
Rodell, M. *et al.*, 2004. The global land data assimilation system, *Bull. Am. Meteorol. Soc.,* **85,** 381–394.
Rodell, M., Velicogna, I. & Famiglietti, J.S., 2009. Satellite-based estimates of groundwater depletion in India, *Nature,* **460,** 999–1002.
Scanlon, B.R., Longuevergne, L. & Long, D., 2012. Ground referencing GRACE satellite estimates of groundwater storage changes in the California Central Valley, USA, *Water Resour. Res.,* **48,** 4520, doi:10.1029/2011WR011312.
Schneider, U., Becker, A., Finger, P., Meyer-Christoffer, A., Ziese, M. & Rudolf, B., 2014. GPCC's new land surface precipitation climatology based on quality-controlled in situ data and its role in quantifying the global water cycle, *Theor. Appl. Climatol.,* **115,** 15–40.
Song, C. & Sheng, Y., 2016. Contrasting evolution patterns between glacier-fed and non-glacier-fed lakes in the Tanggula Mountains and climate cause analysis, *Clim. Change,* **135**(3), 493–507.
Song, C., Huang, B. & Ke, L., 2013. Modeling and analysis of lake water storage changes on the Tibetan Plateau using multi-mission satellite data, *Remote Sens. Environ.,* **135,** 25–35.
Song, C., Huang, B., Richards, K., Ke, L. & Phan, V.H., 2014. Accelerated lake expansion on the Tibetan Plateau in the 2000s: induced by glacial melting or other processes?, *Water Resour. Res.,* **50,** 3170–3186.
Song, C., Ke, L., Huang, B. & Richards, K.S., 2015. Can mountain glacier melting explains the grace-observed mass loss in the southeast Tibetan plateau: from a climate perspective?, *Global Planet. Change,* **124,** 1–9.
Sun, W., Wang, Q., Li, H., Wang, Y., Okubo, S., Shao, D., Liu, D. & Fu, G., 2009. Gravity and GPS measurements reveal mass loss beneath the Tibetan Plateau: geodetic evidence of increasing crustal thickness, *Geophys. Res. Lett.,* **36,** L02303, doi:10.1029/2008GL036512.
Swenson, S. & Wahr, J., 2002. Methods for inferring regional surface mass anomalies from GRACE measurements of time-variable gravity, *J. geophys. Res.,* **107**(B9), 2193, doi:10.1029/2001JB000576.
Swenson, S. & Wahr, J., 2009. Monitoring the water balance of Lake Victoria, East Africa, from space, *J. Hydrol.,* **370,** 163–176.
Swenson, S., Chambers, D. & Wahr, J., 2008. Estimating geocenter variations from a combination of GRACE and ocean model output, *J. geophys. Res.,* **113,** B08410, doi:10.1029/2007JB005338.
Syed, T.H., Famiglietti, J.S., Rodell, M., Chen, J. & Wilson, C.R., 2008. Analysis of terrestrial water storage changes from GRACE and GLDAS, *Water Resour. Res.,* **44,** W02433, doi:10.1029/2006WR005779.
Tapley, B.D., Bettadpur, S., Ries, J.C., Thompson, P.F. & Watkins, M.M., 2004. GRACE measurements of mass variability in the Earth system, *Science,* **305,** 503–505.
Tapponnier, P., Zhiqin, X., Roger, F., Meyer, B., Arnaud, N., Wittlinger, G. & Jingsui, Y., 2001. Oblique stepwise rise and growth of the Tibet Plateau, *Science,* **294**(5547), 1671–1677.
Unger-Shayesteh, K., Vorogushyn, S., Farinotti, D., Gafurov, A., Duethmann, D., Mandychev, A. & Merz, B., 2013. What do we know about past changes in the water cycle of Central Asian headwaters? A review, *Global Planet. Change,* **110,** 4–25.
van Dam, T., Wahr, J. & Lavallée, D., 2007. A comparison of annual vertical crustal displacements from GPS and Gravity Recovery and Climate Experiment (GRACE) over Europe, *J. geophys. Res.,* **112,** B03404, doi:10.1029/2006JB004335.
Wahr, J., Molenaar, M. & Bryan, F., 1998. Time-variability of the earth's gravity field: hydrological and oceanic effects and their possible detection using GRACE, *J. geophys. Res.,* **103,** 30205–30230.
Wahr, J., Smeed, D.A., Leuliette, E. & Swenson, S., 2014. Seasonal variability of the Red Sea, from satellite gravity, radar altimetry, and in situ observations, *J. geophys. Res.,* **119,** 5091–5104.
Wang, Q., Yi, S. & Sun, W., 2016. The changing pattern of lake and its contribution to increased mass in the Tibetan Plateau derived from GRACE and ICESat data, *Geophys. J. Int.,* **207,** 528–541.
Wang, X., de Linage, C., Famiglietti, J. & Zender, C.S., 2011. Gravity Recovery and Climate Experiment (GRACE) detection of water storage changes in the Three Gorges Reservoir of China and comparison with in situ measurements, *Water Resour. Res.,* **47,** W12502, doi:10.1029/2011WR010534.
Wang, X. *et al.*, 2013. Water-level changes in China's large lakes determined from ICESat/GLAS data, *Remote Sens. Environ.,* **132,** 131–144.

Yang, K., Wu, H., Qin, J., Lin, C., Tang, W. & Chen, Y., 2013. Recent climate changes over the Tibetan Plateau and their impacts on energy and water cycle: a review, *Global Planet. Change,* **112,** 79–91.

Yang, K., Ye, B., Zhou, D., Wu, B., Foken, T., Qin, J. & Zhou, Z., 2011. Response of hydrological cycle to recent climate changes in the Tibetan Plateau, *Clim. Change,* **109**(3–4), 517–534.

Yao, T., Pu, J., Lu, A., Wang, Y. & Yu, W., 2007. Recent glacial retreat and its impact on hydrological processes on the Tibetan Plateau, China, and surrounding regions, *Arct. Antarct. Alp. Res.,* **39**(4), 642–650.

Ye, Q.H., Zhu, L.P., Zheng, H.P., Naruse, R.J., Zhang, X.Q. & Kang, S.C., 2007. Glacier and lake variations in the Yamzhog Yumco basin, southern Tibetan Plateau, from 1980 to 2000 using remote-sensing and GIS technologies, *J. Glaciol.,* **53**(183), 673–676.

Yi, S. & Sun, W., 2014. Evaluation of glacier changes in high-mountain Asia based on 10 year GRACE RL05 models, *J. geophys. Res.,* **119**(3), 2504–2517.

Yi, S., Freymueller, J.T. & Sun, W., 2016b. How fast is the middle-lower crust flowing in eastern Tibet? A constraint from geodetic observations, *J. geophys. Res.,* **121,** 6903–6915.

Yi, S., Song, C., Wang, Q., Wang, L., Heki, K. & Sun, W., 2017. The potential of GRACE gravimetry to detect the heavy rainfall-induced impoundment of a small reservoir in the upper Yellow River, *Water Resour. Res.,* **53,** 6562–6578.

Yi, S., Wang, Q. & Sun, W., 2016a. Is it possible that a gravity increase of 20 μGal yr^{-1} in southern Tibet comes from a wide-range density increase?, *Geophys. Res. Lett.,* **43,** 1481–1486.

You, Q., Kang, S., Pepin, N. & Yan, Y., 2008. Relationship between trends in temperature extremes and elevation in the eastern and central Tibetan Plateau, 1961–2005, *Geophys. Res. Lett.,* **35**(4), L04704, doi:10.1029/2007GL032669.

Zhang, G., Xie, H., Duan, S., Tian, M. & Yi, D., 2011b. Water level variation of Lake Qinghai from satellite and in situ measurements under climate change, *J. appl. Remote Sens.,* **5**(1), 53,532–53,532.

Zhang, G., Xie, H., Kang, S., Yi, D. & Ackley, S.F., 2011a. Monitoring lake level changes on the Tibetan Plateau using ICESat altimetry data (2003–2009), *Remote Sens. Environ.,* **115**(7), 1733–1742.

Zhang, G., Yao, T., Xie, H., Kang, S. & Lei, Y., 2013. Increased mass over the Tibetan Plateau: from lakes or glaciers?, *Geophys. Res. Lett.,* **40,** 2125–2130.

Zhang, T. & Jin, S., 2013. Estimate of glacial isostatic adjustment uplift rate in the Tibetan Plateau from GRACE and GIA models, *J. Geodyn.,* **72,** 59–66.

Zhu, L., Xie, M. & Wu, Y., 2010. Quantitative analysis of lake area variations and the influence factors from 1971 to 2004 in the Nam Co basin of the Tibetan Plateau, *Chin. Sci. Bull.,* **55**(13), 1294–1303.

SUPPORTING INFORMATION

Supplementary data are available at *GJI* online.

Table S1: Sources of data used in this study.
Table S2: News reports about water level and volume changes in Longyangxia Reservoir.

Please note: Oxford University Press is not responsible for the content or functionality of any supporting materials supplied by the authors. Any queries (other than missing material) should be directed to the corresponding author for the paper.